

QCD with overlap fermions: Running coupling and the 3-loop β -function

M. Constantinou, H. Panagopoulos
*Department of Physics, University of Cyprus,
P.O.Box 20537, Nicosia CY-1678, Cyprus
email: phpgmc1@ucy.ac.cy, haris@ucy.ac.cy*

Abstract

We calculate the relation between the bare coupling constant g_0 and the $\overline{\text{MS}}$ -renormalized coupling $g_{\overline{\text{MS}}}$, $g_0 = Z_g(g_0, a\mu)g_{\overline{\text{MS}}}$, to 2 loops in perturbation theory. We employ the standard Wilson action for gluons and the overlap action for fermions. For convenience, we have worked with the background field technique, which only requires evaluation of 2-point Green's function for the problem at hand. Our results depend explicitly on the number of fermion flavors (N_f) and colors (N). Since the dependence of Z_g on the overlap parameter ρ cannot be extracted analytically, we tabulate our results for different values in the allowed range of ρ ($0 < \rho < 2$), focusing on values which are being used most frequently in simulations. Knowledge of Z_g allows us to derive the 3-loop coefficient of the bare β -function ($\beta_L(g_0)$) which, unlike the 1- and 2-loop coefficients, is regularization-dependent. The nontrivial dependence of Z_g and of $\beta_L(g_0)$ on ρ is plotted for various choices of N , N_f .

Keywords: Beta function, Overlap fermions, Running coupling constant, Lattice perturbation theory.

PACS numbers: 11.15.Ha, 12.38.Gc, 12.38.Bx, 11.10.Gh.

I. INTRODUCTION

In later years, use of non-ultralocal actions which preserve chiral symmetry on the lattice has become more viable. The two actions which are being used most frequently are overlap fermions [1–3] based on the Wilson fermion action and domain-wall fermions [4,5].

Overlap fermions are notoriously difficult to study, both numerically and analytically. Many recent promising investigations involving simulations with overlap fermions have appeared; see, e.g., Refs. [6–12]. Regarding analytical computations, the only ones performed thus far have been either up to 1 loop, such as Refs. [13–19], or vacuum diagrams at higher loops [20,21]. *The present work is the first one involving non-vacuum diagrams beyond the 1-loop level.*

We compute the 2-loop renormalization Z_g of the bare lattice coupling constant g_0 in the presence of overlap fermions. We relate g_0 to the renormalized coupling constant $g_{\overline{\text{MS}}}$ as defined in the $\overline{\text{MS}}$ scheme at a scale $\bar{\mu}$; at large momenta, these quantities are related as follows

$$\alpha_{\overline{\text{MS}}}(\bar{\mu}) = \alpha_0 + d_1(\bar{\mu}a)\alpha_0^2 + d_2(\bar{\mu}a)\alpha_0^3 + \dots, \quad (1)$$

($\alpha_0 = g_0^2/4\pi$, $\alpha_{\overline{\text{MS}}} = g_{\overline{\text{MS}}}^2/4\pi$, a : lattice spacing). The 1-loop coefficient $d_1(\bar{\mu}a)$ has been known for a long time; several evaluations of $d_2(\bar{\mu}a)$ have also appeared in the past ~ 10 years, either in the absence of fermions [22,23], or using the Wilson [24] or clover [25,26] fermionic actions. Knowledge of $d_2(\bar{\mu}a)$, along with the 3-loop $\overline{\text{MS}}$ -renormalized β -function [27] allows us to derive the 3-loop bare lattice β -function, which dictates the dependence of lattice spacing on g_0 . In particular, it provides a correction to the standard 2-loop asymptotic scaling formula defining Λ_L . Ongoing efforts to estimate the running coupling from the lattice [28–31] have relied on a mixture of perturbative and non-perturbative investigations. As a particular example, relating $\alpha_{\overline{\text{MS}}}$ to α_{SF} (SF: Schrödinger Functional scheme, as advocated by the ALPHA Collaboration), entails an intermediate passage through the bare coupling and the conversion from $\alpha_{\overline{\text{MS}}}$ to α_0 is carried out perturbatively.

The paper is organized as follows: Some theoretical background and the methodology of the necessary perturbative calculations are given in Section II. Section III regards the overlap action where the derivation of the vertices with up to 4 gluons is explained. We also provide the expressions for these vertices (the 4-gluon vertex is given in Appendix A). Details on our computation, numerical results and plots of Z_g coefficients and the β -function can be found in Section IV. Finally, in Section V we give the summary and our conclusions.

The present study, being the first of its kind in calculating 2-loop diagrams with overlap vertices and external momentum dependence, had a number of obstacles to overcome. One first complication is the size of the algebraic form of the Feynman vertices; as an example, the vertex with 4 gluons and a fermion-antifermion pair contains $\sim 724,000$ terms when expanded. Upon contraction these vertices lead to huge expressions (many millions of terms); this places severe requirements both on the efficiency of the computer algorithms which we must design to manipulate such expressions automatically and on the necessary computer RAM. Numerical integration of Feynman diagrams over loop momentum variables is performed on a range of lattices, with finite size L , and subsequent extrapolation to $L \rightarrow \infty$. As it turned out, larger L were required for an accurate extrapolation in the present case, compared to ultra-local actions. In addition, since the results depend nontrivially on the

parameter ρ of the overlap action, numerical evaluation must be performed for a sufficiently wide set of values of ρ , with an almost proportionate increase in CPU time. Extreme values of ρ ($\rho \gtrsim 0$, $\rho \lesssim 2$) show unstable numerical behaviour, which is attributable to the spurious poles of the fermion propagator at these choices; this forces us to even larger L . A consequence of all complications noted above is an extended use of CPU time: Our numerical integration codes, which ran on a 32-node cluster of dual CPU Pentium IV processors, required a total of ~ 50 years of CPU time.

II. THEORETICAL BACKGROUND

The definition and value of the renormalized coupling constant g depends on the renormalization scheme (parameterized by a scale μ), and this dependence is given by the renormalized β -function

$$\beta(g) \equiv \mu \frac{dg}{d\mu} \quad (2)$$

We will adopt the $\overline{\text{MS}}$ renormalization scheme throughout this work, and we will denote the renormalized coupling constant $g_{\overline{\text{MS}}}$ simply by g . For the lattice regularization a bare β -function is defined as

$$\beta_L(g_0) = -a \left. \frac{dg_0}{da} \right|_{g, \bar{\mu}} \quad (3)$$

where $\bar{\mu}$ the renormalization scale and g (g_0) the renormalized (bare) coupling constant. It is well known that in the asymptotic limit for QCD ($g_0 \rightarrow 0$), one can write the expansion of the β -function in powers of g_0 , that is

$$\beta_L(g_0) = -b_0 g_0^3 - b_1 g_0^5 - b_2^L g_0^7 - \dots \quad (4)$$

The coefficients b_0, b_1 are universal constants (regularization independent) given by

$$\begin{aligned} b_0 &= \frac{1}{(4\pi)^2} \left(\frac{11}{3} N - \frac{2}{3} N_f \right) \\ b_1 &= \frac{1}{(4\pi)^4} \left[\frac{34}{3} N^2 - N_f \left(\frac{13}{3} N - \frac{1}{N} \right) \right] \end{aligned} \quad (5)$$

where $N(N_f)$ is the number of colors (flavors).

On the contrary, b_i^L ($i \geq 2$) depends on the regulator; it must be determined perturbatively. In the present work we calculate the coefficient b_2^L using the overlap fermionic action and Wilson gluons.

The perturbative expansion of the renormalized β -function is

$$\beta(g) = \bar{\mu} \left. \frac{dg}{d\bar{\mu}} \right|_{a, g_0} = -b_0 g^3 - b_1 g^5 - b_2 g^7 + \dots \quad (6)$$

$\beta_L(g_0)$ and $\beta(g)$ can be related using the renormalization function Z_g , defined through $g_0 = Z_g(g_0, a\bar{\mu})g$, that is ¹

$$\beta^L(g_0) = \left(1 - g_0^2 \frac{\partial \ln Z_g^2}{\partial g_0^2}\right)^{-1} Z_g \beta(g_0 Z_g^{-1}) \quad (7)$$

Computing Z_g^2 to 2 loops

$$Z_g^2(g_0, a\bar{\mu}) = 1 + g_0^2 (2b_0 \ln(a\bar{\mu}) + l_0) + g_0^4 (2b_1 \ln(a\bar{\mu}) + l_1) + O(g_0^6) \quad (8)$$

and inserting it in Eq. (7), allows us to extract the 3-loop coefficient b_2^L . The quantities b_0, b_1, b_2 and l_0 have been known in the literature for quite some time [27,19]; b_0 and b_1 are the same as those of the bare β -function, Eq. (5), and b_2 in the $\overline{\text{MS}}$ scheme is

$$b_2 = \frac{1}{(4\pi)^6} \left[\frac{2857}{54} N^3 + N_f \left(-\frac{1709N^2}{54} + \frac{187}{36} + \frac{1}{4N^2} \right) + N_f^2 \left(\frac{56N}{27} - \frac{11}{18N} \right) \right] \quad (9)$$

The constant l_0 is related to the ratio of the Λ parameters associated with the particular lattice regularization and the $\overline{\text{MS}}$ renormalization scheme

$$l_0 = 2b_0 \ln(\Lambda_L/\Lambda_{\overline{\text{MS}}}) \quad (10)$$

For overlap fermions the exact form of l_0 appears in Ref. [19]

$$l_0 = \frac{1}{8N} - 0.16995599N + N_f \left[-\frac{5}{72\pi^2} - k(\rho) \right] \quad (11)$$

where $k(\rho)$ is the convergent part of the 1-loop fermionic contribution (denoted by $k_f(\rho)$ in Ref. [19]), presented in Table I.

Eq. (7) is valid order by order in perturbation theory and expanding it in powers of g_0^2 the first nontrivial relation is

$$b_2^L = b_2 - b_1 l_0 + b_0 l_1 \quad (12)$$

Thus, the evaluation of b_2^L requires only the determination of the 2-loop quantity l_1 .

A direct outcome of our calculation is the 2-loop corrected asymptotic scaling relation between a and g_0

$$a = \frac{1}{\Lambda_L} \exp\left(-\frac{1}{2b_0 g_0^2}\right) (b_0 g_0^2)^{-b_1/2b_0^2} \left[1 + q g_0^2 + \mathcal{O}(g_0^4)\right], \quad q = \frac{b_1^2 - b_0 b_2^L}{2b_0^3} \quad (13)$$

where all quantities in the correction term q , except b_2^L , are known.

The most convenient and economical way to proceed with calculating $Z_g(g_0, a\bar{\mu})$ is to use the background field technique [32,33,23], in which the following relation is valid

¹ Z_g could be denoted: $Z_g^{L, \overline{\text{MS}}}$ to indicate its dependence on the regulator (L : lattice) and on the renormalization scheme ($\overline{\text{MS}}$).

$$Z_A(g_0, a\bar{\mu})Z_g^2(g_0, a\bar{\mu}) = 1 \quad (14)$$

where Z_A , defined as: $A^\mu(x) = Z_A(g_0, a\bar{\mu})^{1/2}A_R^\mu(x)$ is the background field renormalization function (A^μ (A_R^μ): bare (renormalized) background field). In the lattice version of the background field technique, the link variable takes the form

$$U_\mu(x) = e^{ia g_0 Q_\mu(x)} \cdot e^{ia A_\mu(x)} \quad (15)$$

($Q_\mu(x)$: quantum field, $A_\mu(x)$: background field). In this framework, instead of $Z_g(g_0, a\bar{\mu})$, it suffices to compute $Z_A(g_0, a\bar{\mu})$, with no need to evaluate any 3-point functions. For this purpose, we consider the background field one-particle irreducible (1PI) 2-point function, both in the continuum (dimensional regularization, $\overline{\text{MS}}$ subtraction): $\Gamma_R^{AA}(p)_{\mu\nu}^{ab}$ and on the lattice: $\Gamma_L^{AA}(p)_{\mu\mu}^{ab}$. In the notation of Ref. [23], these 2-point functions can be expressed in terms of scalar functions $\nu_R(p)$, $\nu(p)$

$$\Gamma_R^{AA}(p)_{\mu\nu}^{ab} = -\delta^{ab} (\delta_{\mu\nu} p^2 - p_\mu p_\nu) (1 - \nu_R(p)) / g^2, \quad \nu_R(p) = g^2 \nu_R^{(1)}(p) + g^4 \nu_R^{(2)}(p) + \dots \quad (16)$$

$$\sum_\mu \Gamma_L^{AA}(p)_{\mu\mu}^{ab} = -\delta^{ab} 3\hat{p}^2 [1 - \nu(p)] / g_0^2, \quad \nu(p) = g_0^2 \nu^{(1)}(p) + g_0^4 \nu^{(2)}(p) + \dots \quad (17)$$

($\hat{p}_\mu = (2/a) \sin(ap_\mu/2)$). There follows

$$Z_A = \frac{1 - \nu_R(p, \bar{\mu}, g)}{1 - \nu(p, a, g_0)} \quad (18)$$

The gauge parameter λ must also be renormalized (up to 1 loop), in order to compare lattice and continuum results

$$\lambda = Z_Q \lambda_0, \quad Z_Q = 1 + g_0^2 z_Q^{(1)} + \dots \quad (19)$$

(Z_Q : renormalization function of the quantum field). The coefficient $z_Q^{(1)}$ is obtained from the quantum field 1PI 2-point function in the continuum ($\Gamma_R^{QQ}(p)_{\mu\nu}^{ab}$) and on the lattice ($\Gamma_L^{QQ}(p)_{\mu\nu}^{ab}$) through

$$\Gamma_R^{QQ}(p)_{\mu\nu}^{ab} = -\delta^{ab} [(\delta_{\mu\nu} p^2 - p_\mu p_\nu) (1 - \omega_R(p)) + \lambda p_\mu p_\nu], \quad \omega_R(p) = g^2 \omega_R^{(1)}(p) + \mathcal{O}(g^4) \quad (20)$$

$$\sum_\mu \Gamma_L^{QQ}(p)_{\mu\mu}^{ab} = -\delta^{ab} \hat{p}^2 [3(1 - \omega(p)) + \lambda_0], \quad \omega(p) = g_0^2 \omega^{(1)}(p) + \mathcal{O}(g_0^4) \quad (21)$$

$$z_Q^{(1)} = \omega^{(1)}(p, a, g_0) - \omega_R^{(1)}(p, \bar{\mu}, g) \quad (22)$$

In terms of the perturbative expansions Eqs. (16), (17), (20), (21), Z_g^2 takes the form

$$Z_g^2 = \left[1 + g_0^2 (\nu_R^{(1)} - \nu^{(1)}) + g_0^4 (\nu_R^{(2)} - \nu^{(2)}) + \lambda_0 g_0^4 (\omega^{(1)} - \omega_R^{(1)}) \frac{\partial \nu_R^{(1)}}{\partial \lambda} \right]_{\lambda=\lambda_0} \quad (23)$$

The fermion part of $\omega^{(1)}$ coincides with that of $\nu^{(1)}$. Similarly for the fermion part of $\omega_R^{(1)}$ and $\nu_R^{(1)}$. Consequently, one may write

$$\omega^{(1)} - \omega_R^{(1)} = [\omega^{(1)} - \omega_R^{(1)}]_{N_f=0} + [\nu^{(1)} - \nu_R^{(1)}] - [\nu^{(1)} - \nu_R^{(1)}]_{N_f=0} \quad (24)$$

Since the quantities of interest are gauge invariant, we choose to work in the bare Feynman gauge, $\lambda_0 = 1$, for convenience. In order to compute Z_A we need the expressions for $\nu_R^{(1)}$, $\nu_R^{(2)}$, $z_Q^{(1)}$, $\nu^{(1)}$, $\nu^{(2)}$. The $\overline{\text{MS}}$ renormalized functions necessary for this calculation to 2 loops are [23,34]

$$\nu_R^{(1)}(p, \lambda) = \frac{N}{16\pi^2} \left[-\frac{11}{3} \ln \frac{p^2}{\bar{\mu}^2} + \frac{205}{36} + \frac{3}{2\lambda} + \frac{1}{4\lambda^2} \right] + \frac{N_f}{16\pi^2} \left[\frac{2}{3} \ln \frac{p^2}{\bar{\mu}^2} - \frac{10}{9} \right] \quad (25)$$

$$\omega_R^{(1)}(p, \lambda) = \frac{N}{16\pi^2} \left[\left(-\frac{13}{6} + \frac{1}{2\lambda} \right) \ln \frac{p^2}{\bar{\mu}^2} + \frac{97}{36} + \frac{1}{2\lambda} + \frac{1}{4\lambda^2} \right] + \frac{N_f}{16\pi^2} \left[\frac{2}{3} \ln \frac{p^2}{\bar{\mu}^2} - \frac{10}{9} \right] \quad (26)$$

$$\begin{aligned} \nu_R^{(2)}(p, \lambda = 1) &= \frac{N^2}{(16\pi^2)^2} \left[-8 \ln \frac{p^2}{\bar{\mu}^2} + \frac{577}{18} - 6\zeta(3) \right] + \\ &\quad \frac{N_f}{(16\pi^2)^2} \left[N \left(3 \ln \frac{p^2}{\bar{\mu}^2} - \frac{401}{36} \right) + \frac{1}{N} \left(-\ln \frac{p^2}{\bar{\mu}^2} + \frac{55}{12} - 4\zeta(3) \right) \right] \end{aligned} \quad (27)$$

For the lattice quantities, the gluonic contributions ($N_f = 0$) have been presented in previous works [23,34] (for the Wilson action)

$$\omega^{(1)}(p, \lambda_0 = 1) = -\frac{5N}{48\pi^2} \ln(a^2 p^2) - \frac{1}{8N} + 0.137286278291N \quad (28)$$

$$\nu^{(1)}(p, \lambda_0 = 1) = -\frac{11N}{48\pi^2} \ln(a^2 p^2) - \frac{1}{8N} + 0.217098494367N \quad (29)$$

$$\nu^{(2)}(p, \lambda_0 = 1) = -\frac{N}{32\pi^4} \ln(a^2 p^2) + \frac{3}{128N^2} - 0.01654461954 + 0.0074438722N^2 \quad (30)$$

The fermionic contributions are associated with the diagrams of Fig. 1 and Fig. 2. In the present work, $\nu^{(2)}$ is perturbatively calculated for the first time using overlap fermions and Wilson gluons. For completeness, we also compute the coefficient $\nu^{(1)}$ and compare it with previous results. The 1-loop diagrams (Fig. 1) correspond to $\nu^{(1)}$, while the 2-loop diagrams (Fig. 2) lead to $\nu^{(2)}$. Dashed lines ending in a cross represent the background field, while those inside loops denote the quantum field. Solid lines correspond to fermion fields and a dot stands for the mass counterterm. Note that, for overlap fermions, the mass counterterm equals zero, by virtue of the exact chiral symmetry of the overlap action; consequently, diagrams 19 and 20 both vanish. Certain 2-loop diagrams have infrared divergences and become convergent only when grouped together (6+12, 7+11, 8+18, 9+17).

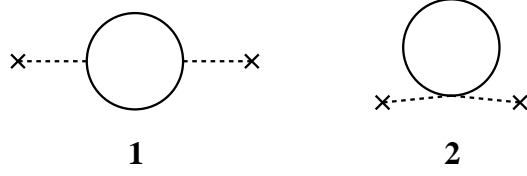


Fig. 1: Fermion contributions to the 1-loop function $\nu^{(1)}$. Dashed lines ending on a cross represent background gluons. Solid lines represent fermions.

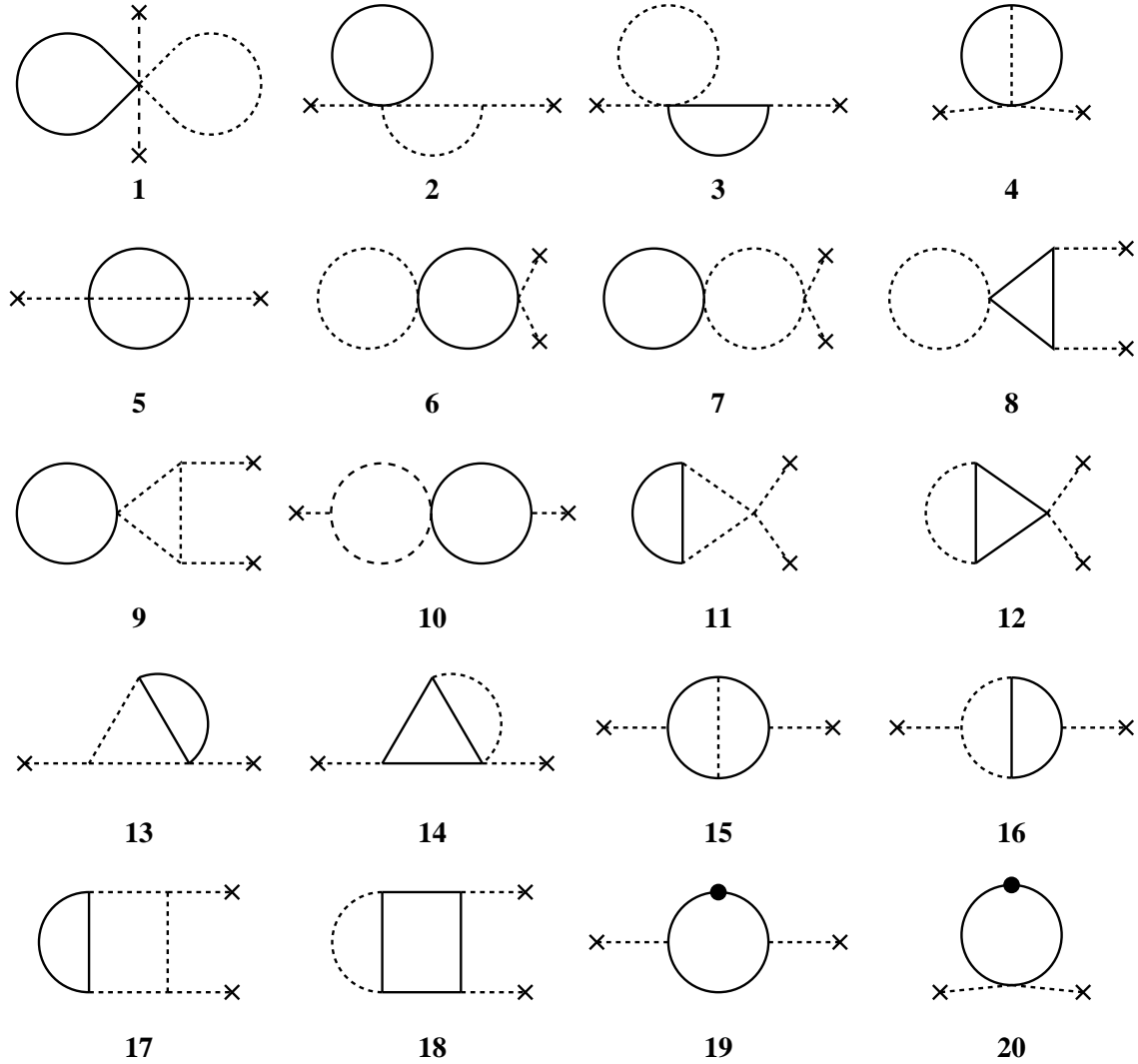


Fig. 2: Fermion contributions to the 2-loop function $\nu^{(2)}$. Dashed lines represent gluonic fields; those ending on a cross stand for background gluons. Solid lines represent fermions. The filled circle is a 1-loop fermion mass counterterm.

III. OVERLAP ACTION

In recent years, overlap fermions are being used ever more extensively in numerical simulations, both in the quenched approximation and beyond. This fact, along with the desirable properties of the overlap action, was our motivation to calculate the β -function with this type of fermions. The important advantage of the overlap action is that it preserves chiral symmetry while avoiding fermion doubling. It is also $\mathcal{O}(a)$ improved. The main drawback of this action is that it is necessarily non-ultralocal; as a consequence, both numerical simulations and perturbative studies are extremely difficult and demanding (in terms of human, as well as computer time).

The overlap action is given by [2]

$$S_{\text{overlap}} = a^8 \sum_{n,m} \bar{\Psi}(n) D_N(n, m) \Psi(m) \quad (31)$$

where $D_N(n, m)$ is the overlap-Dirac operator

$$D_N(n, m) = \rho \left[\frac{\delta_{n,m}}{a^4} - \left(X \frac{1}{\sqrt{X^\dagger X}} \right)_{nm} \right], \quad X = \frac{1}{a^4} (D_W - \rho) \quad (32)$$

and D_W is the Wilson-Dirac operator

$$D_W = \frac{1}{2} \left[\gamma_\mu (\nabla_\mu^* + \nabla_\mu) - a \nabla_\mu^* \nabla_\mu \right], \quad \nabla_\mu \psi(x) = \frac{1}{a} [U(x, \mu) \psi(x + a\hat{\mu}) - \psi(x)] \quad (33)$$

The overlap parameter ρ is restricted by the condition $0 < \rho < 2$ to guarantee the correct pole structure of D_N . The coupling constant is included in the link variables, present in the definition of X , and one must take the perturbative expansion of X in powers of g_0 . This expansion in momentum space takes the form

$$X(p', p) = \underbrace{\chi_0(p)(2\pi)^4 \delta_P(p' - p)}_{\text{tree-level}} + \underbrace{X_1(p', p) + X_2(p', p)}_{\text{1-loop}} + \underbrace{X_3(p', p) + X_4(p', p)}_{\text{2-loop}} + O(g_0^5) \quad (34)$$

where χ_0 is the inverse fermion propagator and X_i are the vertices of the Wilson fermion action (p (p'): fermion (antifermion) momentum). The construction of all overlap vertices relevant to the present computation (see Eqs. (39), (40), (41), (42), (A7) below) make use of χ_0 and $X_1 - X_4$; these quantities can be written in the compact form

$$\begin{aligned} \chi_0(p) &= \frac{i}{a} \sum_\mu \gamma_\mu \sin(ap_\mu) + \frac{r}{a} \sum_\mu (1 - \cos(ap_\mu)) - \frac{\rho}{a} \\ X_1(p', p) &= g_0 \int d^4 k \delta(p' - p - k) \sum_\mu A_\mu(k) V_{1,\mu} \left(\frac{p' + p}{2} \right) \\ X_2(p', p) &= \frac{g_0^2}{2} \int \frac{d^4 k_1 d^4 k_2}{(2\pi)^4} \delta(p' - p - k_1 - k_2) \sum_\mu A_\mu(k_1) A_\mu(k_2) V_{2,\mu} \left(\frac{p' + p}{2} \right) \\ X_3(p', p) &= \frac{g_0^3}{3!} \int \frac{d^4 k_1 d^4 k_2 d^4 k_3}{(2\pi)^8} \delta(p' - p - \sum_{i=1}^3 k_i) \sum_\mu \prod_{i=1}^3 A_\mu(k_i) \left[-a^2 V_{1,\mu} \left(\frac{p' + p}{2} \right) \right] \\ X_4(p', p) &= \frac{g_0^4}{4!} \int \frac{d^4 k_1 d^4 k_2 d^4 k_3 d^4 k_4}{(2\pi)^{12}} \delta(p' - p - \sum_{i=1}^4 k_i) \sum_\mu \prod_{i=1}^4 A_\mu(k_i) \left[-a^2 V_{2,\mu} \left(\frac{p' + p}{2} \right) \right] \end{aligned} \quad (35)$$

where

$$V_{1,\mu}(p) = i \gamma_\mu \cos(ap_\mu) + r \sin(ap_\mu), \quad V_{2,\mu}(p) = -i \gamma_\mu a \sin(ap_\mu) + a r \cos(ap_\mu) \quad (36)$$

A_μ represents a gluon field; later on we will have to generalize Eqs. (35) to the case where both background and quantum gluon field are present, see Eq. (43).

At this point we can proceed with the perturbative expansion of D_N in powers of g_0 . This leads to the propagator of zero mass fermions and to gluon-fermion-antifermion vertices (with up to 4 gluons for the needs of the present work). The much simpler case of vertices with up to 2 gluons (and no background) can be found in Ref. [35]. After laborious analytical manipulations (an essential step is the expansion of $1/\sqrt{X^\dagger X}$ using complex analysis, which is presented in Appendix A), the overlap-Dirac operator is expanded into terms with up to 4 gluons as

$$D_N(k_1, k_2) = D_0(k_1) (2\pi)^4 \delta^4(k_1 - k_2) + \Sigma(k_1, k_2) \quad (37)$$

$D_0(k_1)$ is the inverse propagator,

$$D_0(k_1) = 1 + \frac{\chi_0(k_1)}{\omega(k_1)}, \quad \omega(p) = \sqrt{\left(\sum_\mu \sin^2(p_\mu)\right) + \left(\rho - 2r \sum_\mu \sin^2(p_\mu/2)\right)^2} \quad (38)$$

and

$$\begin{aligned} \frac{\Sigma(k_1, k_2)}{\rho} = & \underbrace{V_1^1(k_1, k_2)}_{1\text{-gluon vertex}} + \underbrace{V_1^2(k_1, k_2) + V_2^2(k_1, k_2)}_{2\text{-gluon vertex}} \\ & + \underbrace{V_1^3(k_1, k_2) + V_2^3(k_1, k_2) + V_3^3(k_1, k_2)}_{3\text{-gluon vertex}} \\ & + \underbrace{V_1^4(k_1, k_2) + V_2^4(k_1, k_2) + V_3^4(k_1, k_2) + V_4^4(k_1, k_2)}_{4\text{-gluon vertex}} + \mathcal{O}(g_0^5) \end{aligned} \quad (39)$$

where we have set $a = 1$. V_1^i, V_2^i, V_3^i are given below and the reader can find the expression for V_4^i in Appendix A.

$$V_1^i(k_1, k_2) = \frac{1}{\omega(k_1) + \omega(k_2)} \left[X_i(k_1, k_2) - \frac{1}{\omega(k_1)\omega(k_2)} \chi_0(k_1) X_i^\dagger(k_1, k_2) \chi_0(k_2) \right] \quad (40)$$

$$\begin{aligned} V_2^i(k_1, k_2) = & \int \frac{d^4 k_3}{(2\pi)^4} \frac{1}{\omega(k_1) + \omega(k_3)} \frac{1}{\omega(k_1) + \omega(k_2)} \frac{1}{\omega(k_2) + \omega(k_3)} \times \\ & \sum_{\substack{\{j>0, k>0\} \\ \{j+k=i\}}} \left[\begin{aligned} & - X_j(k_1, k_3) \chi_0^\dagger(k_3) X_k(k_3, k_2) \\ & - X_j(k_1, k_3) X_k^\dagger(k_3, k_2) \chi_0(k_2) \\ & - \chi_0(k_1) X_j^\dagger(k_1, k_3) X_k(k_3, k_2) \\ & + \frac{\omega(k_1) + \omega(k_2) + \omega(k_3)}{\omega(k_1)\omega(k_2)\omega(k_3)} \chi_0(k_1) X_j^\dagger(k_1, k_3) \chi_0(k_3) X_k^\dagger(k_3, k_2) \chi_0(k_2) \end{aligned} \right] \end{aligned} \quad (41)$$

$$\begin{aligned}
V_3^i(k_1, k_2) = & \int \int \frac{d^4 k_3}{(2\pi)^4} \frac{d^4 k_4}{(2\pi)^4} \frac{1}{4} \left(\prod_{p \in S_4} \frac{1}{\omega(k_{p_1}) + \omega(k_{p_2})} \right) \times \\
& \sum_{\substack{\{j>0, k>0, l>0\} \\ \{j+k+l=i\}}} \left[-\frac{1}{6} \left(\sum_{p \in S_4} \omega(k_{p_1}) \omega(k_{p_2}) \omega(k_{p_3}) \right) X_j(k_1, k_3) X_k^\dagger(k_3, k_4) X_l(k_4, k_2) \right. \\
& + \left(\omega(k_1) + \omega(k_3) + \omega(k_4) + \omega(k_2) \right) \times \\
& \left[\chi_0(k_1) X_j^\dagger(k_1, k_3) X_k(k_3, k_4) X_l^\dagger(k_4, k_2) \chi_0(k_2) + \chi_0(k_1) X_j^\dagger(k_1, k_3) X_k(k_3, k_4) \chi_0^\dagger(k_4) X_l(k_4, k_2) \right. \\
& + \chi_0(k_1) X_j^\dagger(k_1, k_3) \chi_0(k_3) X_k^\dagger(k_3, k_4) X_l(k_4, k_2) + X_j(k_1, k_3) \chi_0^\dagger(k_3) X_k(k_3, k_4) X_l^\dagger(k_4, k_2) \chi_0(k_2) \\
& \left. \left. + X_j(k_1, k_3) \chi_0^\dagger(k_3) X_k(k_3, k_4) \chi_0^\dagger(k_4) X_l(k_4, k_2) + X_j(k_1, k_3) X_k^\dagger(k_3, k_4) \chi_0(k_4) X_l^\dagger(k_4, k_2) \chi_0(k_2) \right] \right. \\
& \left. - \left(\sum_{p \in S_4} \frac{\omega(k_{p_1}) \omega(k_{p_2}) (\omega(k_{p_1})/2 + \omega(k_{p_3})/3)}{\omega(k_1) \omega(k_3) \omega(k_4) \omega(k_2)} \right) \times \right. \\
& \left. \left. \chi_0(k_1) X_j^\dagger(k_1, k_3) \chi_0(k_3) X_k^\dagger(k_3, k_4) \chi_0(k_4) X_l^\dagger(k_4, k_2) \chi_0(k_2) \right] \right) \quad (42)
\end{aligned}$$

(S_4 : permutation group of the numbers $\{1, 2, 3, 4\}$)

The use of the background field technique implies that instead of the generic gluonic fields (appearing in X_i 's, Eq. (35)), one must consider all possible combinations of background (A) and quantum (Q) fields which originate in the links of Eqs. (33), (15). Hence,

$$\begin{aligned}
X_1(p', p) &= X_1^Q(p', p) + X_1^A(p', p) \\
X_2(p', p) &= X_2^{QQ}(p', p) + X_2^{QA}(p', p) + X_2^{AA}(p', p) \\
X_3(p', p) &= X_3^{QQQ}(p', p) + X_3^{QQA}(p', p) + X_3^{QAA}(p', p) + X_3^{AAA}(p', p) \\
X_4(p', p) &= X_4^{QQQQ}(p', p) + X_4^{QQQA}(p', p) + X_4^{QQA}(p', p) + X_4^{QAAA}(p', p) + X_4^{AAAA}(p', p) \quad (43)
\end{aligned}$$

As an example, let us write the expression for X_3^{QQA}

$$\begin{aligned}
X_3^{QQA}(p', p) &= \frac{g_0^2}{4} \int \frac{d^4 k_1 d^4 k_2 d^4 k_3}{(2\pi)^8} \delta(p' - p - k_1 - k_2 - k_3) \times \\
& \sum_{\mu} \left[-a^2 V_{1,\mu} \left(\frac{p' + p}{2} \right) \left(Q_{\mu}(k_1) Q_{\mu}(k_2) A_{\mu}(k_3) + A_{\mu}(k_3) Q_{\mu}(k_2) Q_{\mu}(k_1) \right) \right. \\
& \left. + ia V_{2,\mu} \left(\frac{p' + p}{2} \right) \left(Q_{\mu}(k_1) Q_{\mu}(k_2) A_{\mu}(k_3) - A_{\mu}(k_3) Q_{\mu}(k_2) Q_{\mu}(k_1) \right) \right] \quad (44)
\end{aligned}$$

Upon substituting the expression for X_i 's in the overlap vertices, the latter become extremely lengthy and complicated. For instance, the vertex with Q-Q-A- Ψ - $\bar{\Psi}$ consists of 9,784 terms, while the vertex with Q-Q-A-A- Ψ - $\bar{\Psi}$ has 724,120 terms.

IV. RESULTS

For the algebra involving lattice quantities, we make use of our symbolic manipulation package in Mathematica, with the inclusion of the additional overlap vertices. The first step

to evaluate the diagrams is the contraction among vertices, a step performed automatically once the vertices and the ‘incidence matrix’ of the diagram are specified. The outcome of contraction is a preliminary expression for the diagram under study; there follow simplifications of the color dependence, Dirac matrices and tensor structures. We use symmetries of the theory (permutation symmetry and lattice rotational invariance), or any other additional symmetry that may appear in particular diagrams, to keep the size of the expression down to a minimum. The external momentum p appears in arguments of trigonometric functions and the extraction of p dependence is divided into two parts: first we isolate terms that give single and double logarithms (a few thousand terms, expressible in terms of known, tabulated integrals), and then for the convergent terms we employ naive Taylor expansion with respect to p up to $\mathcal{O}(p^2)$. This extraction makes explicit the functional dependence of each diagram on p ; the coefficients of terms proportional to p^2 are integrals over the two internal momentum 4-vectors. The required numerical integrations are performed by optimized Fortran programs which are generated by our Mathematica ‘integrator’ routine. Each integral is expressed as a sum over the discrete Brillouin zone of finite lattices, with varying size L , and evaluated for different values of the overlap parameter ρ . The average length of the expression for each diagram, after simplifications, is about 2-3 hundred thousand terms, so that diagrams must be split into parts (usually of 2000 terms) to be integrated. The numerical values of these parts must then be added together to avoid running into systematic errors or spurious divergences. Finally, we extrapolate the results to $L \rightarrow \infty$; this procedure introduces an inherent systematic error, which we can estimate quite accurately. Infrared divergent diagrams must be summed up before performing the extrapolation.

We denote the contribution of the i^{th} 1-loop Feynman diagram to $\nu^{(1)}(p)$ as $\nu_i^{(1)}(p)$; similarly, contributions of 2-loop diagrams to $\nu^{(2)}(p)$ are indicated by $\nu_i^{(2)}(p)$. The quantities $\nu_i^{(1)}(p)$, $\nu_i^{(2)}(p)$ depend on N , N_f , ρ and ap according to the following formulae ($\lambda_0 = 1$)

$$\widehat{ap}^2 \nu_i^{(1)}(p) = N_f \left[k_i^{(0)} + a^2 p^2 \left\{ k_i^{(1)} + k_i^{(2)} \frac{\ln a^2 p^2}{(4\pi)^2} \right\} + \mathcal{O}((ap)^4) \right] \quad (45)$$

$$\widehat{ap}^2 \nu_i^{(2)}(p) = N_f \left[c_i^{(0)} + a^2 p^2 \left\{ c_i^{(1)} + c_i^{(2)} \frac{\ln a^2 p^2}{(4\pi)^2} + c_i^{(3)} \left(\frac{\ln a^2 p^2}{(4\pi)^2} \right)^2 + c_i^{(4)} \frac{\sum_{\mu} p_{\mu}^4}{(p^2)^2} \right\} + \mathcal{O}((ap)^4) \right] \quad (46)$$

where $\widehat{p}^2 = 4 \sum_{\mu} \sin^2(p_{\mu}/2)$. The index i runs over diagrams, and the coefficients $k_i^{(j)}$, $c_i^{(j)}$ depend on the overlap parameter ρ . Moreover, $c_i^{(j)} = [c_i^{(j,-1)}/N + c_i^{(j,1)}N]$. Comparison with continuum results and usage of Ward Identities requires

- $\sum_i k_i^{(0)} = 0, \quad \sum_i c_i^{(0)} = 0 \quad (\text{gauge invariance})$
- $\sum_i k_i^{(2)} = \frac{2}{3}, \quad \sum_i c_i^{(2)} = \frac{1}{16\pi^2} (3N - \frac{1}{N})$
- $\sum_i c_i^{(4)} = 0 \quad (\text{Lorentz invariance})$
- $c_{15}^{(3)} = \frac{1}{3N}, \quad c_{16}^{(3)} = \frac{4}{3}N, \quad c_{17}^{(3)} = -\frac{5}{3}N, \quad c_{18}^{(3)} = \frac{N^2 - 1}{3N} \quad (47)$

We have checked that all the above conditions are verified by our results. Inserting these conditions in Eqs. (45), (46), the expressions for the fermionic contribution to $\nu^{(1)}(p)$, $\nu^{(2)}(p)$ (after addition of all diagrams) take the form

$$\nu^{(1)}(p) = \nu^{(1)}(p)|_{N_f=0} + N_f \left[\sum_i k_i^{(1)} + \frac{2 \ln a^2 p^2}{3 (4\pi)^2} + \mathcal{O}((ap)^2) \right] \quad (48)$$

$$\nu^{(2)}(p) = \nu^{(2)}(p)|_{N_f=0} + N_f \left[\sum_i \left(\frac{c_i^{(1,1)}}{N} + N c_i^{(1,1)} \right) + \frac{1}{16\pi^2} (3N - \frac{1}{N}) \frac{\ln a^2 p^2}{(4\pi)^2} + \mathcal{O}((ap)^2) \right] \quad (49)$$

In Table I we tabulate the total 1-loop contribution $k^{(1)} \equiv \sum_i k_i^{(1)}$ for 21 values of the overlap parameter ($0 < \rho < 2$). Each diagram was integrated for lattice size L^4 , $L \leq 128$ and then extrapolated to $L \rightarrow \infty$. In all Tables and Figures, the errors accompanying our results are entirely due to this extrapolation. The coefficients $k_i^{(1)}(\rho)$ do not depend on the number of colors N , nor on the choice of regularization for the pure gluonic part of the action (Symanzik, Iwasaki, etc.). The numbers in Table I are in agreement with corresponding numbers from Ref. [19].

The 2-loop calculation of $\nu^{(2)}(p)$ was accomplished for the same 21 values of ρ and for $L \leq 28$. Table II presents the coefficients $c^{(1,-1)} \equiv \sum_i c_i^{(1,-1)}$, $c^{(1,1)} \equiv \sum_i c_i^{(1,1)}$, versus ρ . Due to the extremely large size of the vertices involved, it is almost impossible to extend the results to larger L . Typically, the integration of 2000 terms is completed in ~ 7 days on 1 CPU; the present calculation comprises approximately 3500×2000 terms. Thus, if only a single CPU were available, our work would have required ~ 50 years. In certain cases with large systematic errors we extended the integration up to $L = 46$. In general, the overlap action leads to coefficients which are very small for most values of ρ . As a consequence, systematic errors, which are by and large rather small, tend to be significant fractions of the signal for $\rho > 1.4$.

From Eqs. (8), (23)-(28), (30) we find the following expression for l_1 in terms of N , N_f , $k_i^{(1)}$, $c_i^{(1,-1)}$, $c_i^{(1,1)}$

$$l_1 = -\frac{3}{128 N^2} + 0.018127763034 - 0.007910118514 N^2 + N_f \left[\frac{1}{(16\pi^2)^2 N} \left(\frac{55}{12} - 4\zeta(3) \right) - \frac{N}{(16\pi^2)^2} \frac{481}{36} - \frac{N}{8\pi^2} k^{(1)} - \left(\frac{c^{(1,-1)}}{N} + N c^{(1,1)} \right) \right] \quad (50)$$

We can write the final form of the 3-loop coefficient b_2^L for the β -function (Eq. (12)), including gluonic as well as fermionic contributions, using Eqs. (5), (9), (11) and (50)

$$b_2^L = -\frac{11}{2048\pi^2 N} + 0.000364106020 N - 0.000092990690 N^3 + N_f \left[\frac{(4\pi^2 - 1)^2}{4(16\pi^2)^3 N^2} - 0.000046883436 - 000013419574 N^2 + \frac{N_f}{(16\pi^2)^3} \left(-\frac{23}{9N} + \frac{8\zeta(3)}{3N} + \frac{37N}{6} \right) - \frac{(11N - 2N_f)}{48\pi^2} \left(\frac{c^{(1,-1)}}{N} + c^{(1,1)} N \right) + \frac{(4N^3 + N_f - 3N^2 N_f)}{(16\pi^2)^2 N} k^{(1)} \right] \quad (51)$$

A large variety of possible numerical checks has been performed, as mentioned above: **a.** The total contribution to the gluon mass adds to zero, as expected. **b.** The coefficients of the non-Lorentz invariant terms cancel. **c.** The terms with double logarithms correspond to the continuum counterparts. This has been checked diagram by diagram. **d.** Terms with single logarithms add up to their expected value, which is independent of ρ (although the expressions per diagram are ρ -dependent).

In Fig. 3 we plot the 1-loop coefficient $k^{(1)}$ with respect to ρ . Note that the errors are too small to be visible at this scale. The 2-loop coefficients $c^{(1,-1)}$ and $c^{(1,1)}$ are plotted in Figs. 4-5, respectively, for different values of the overlap parameter. The extrapolation errors are visible for $\rho \leq 0.4$ and $\rho \geq 1.7$. Substituting $k^{(1)}$, $c^{(1,-1)}$ and $c^{(1,1)}$ into Eq. (51), we find the numerical results for the 3-loop contribution, b_2^L , of the β -function. These are plotted in Fig. 6, choosing $N = 3$ and $N_f = 0, 2, 3$.

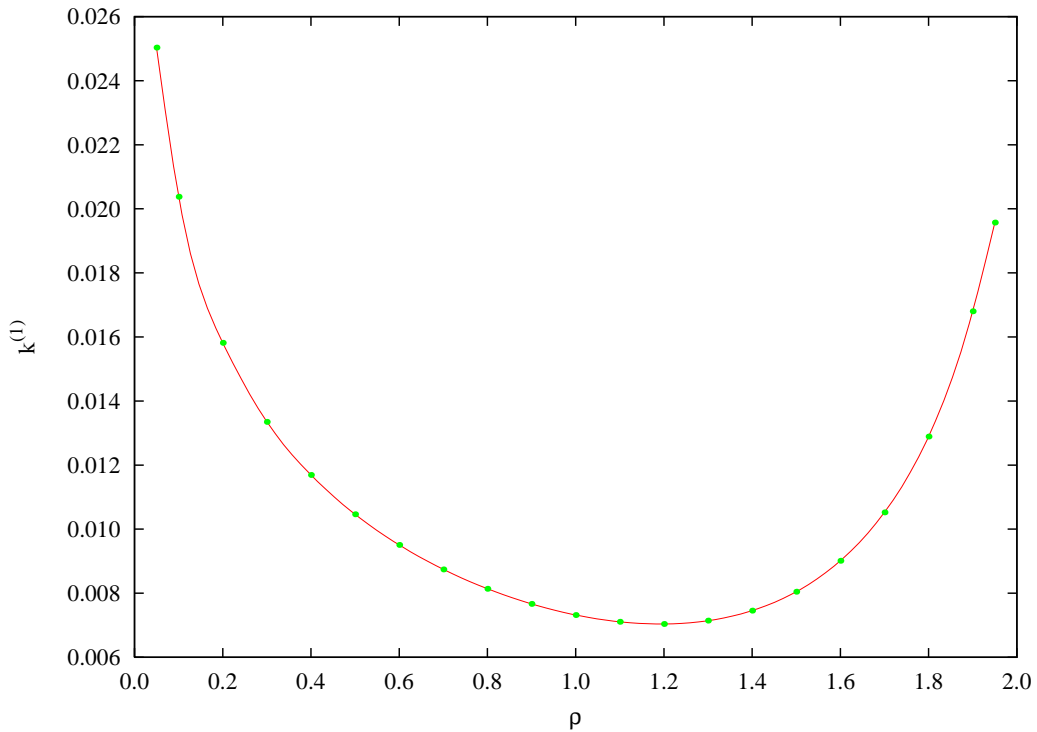


Fig. 3: Plot of the total 1-loop coefficient $k^{(1)} \equiv \sum_i k_i^{(1)}$ versus the overlap parameter ρ .

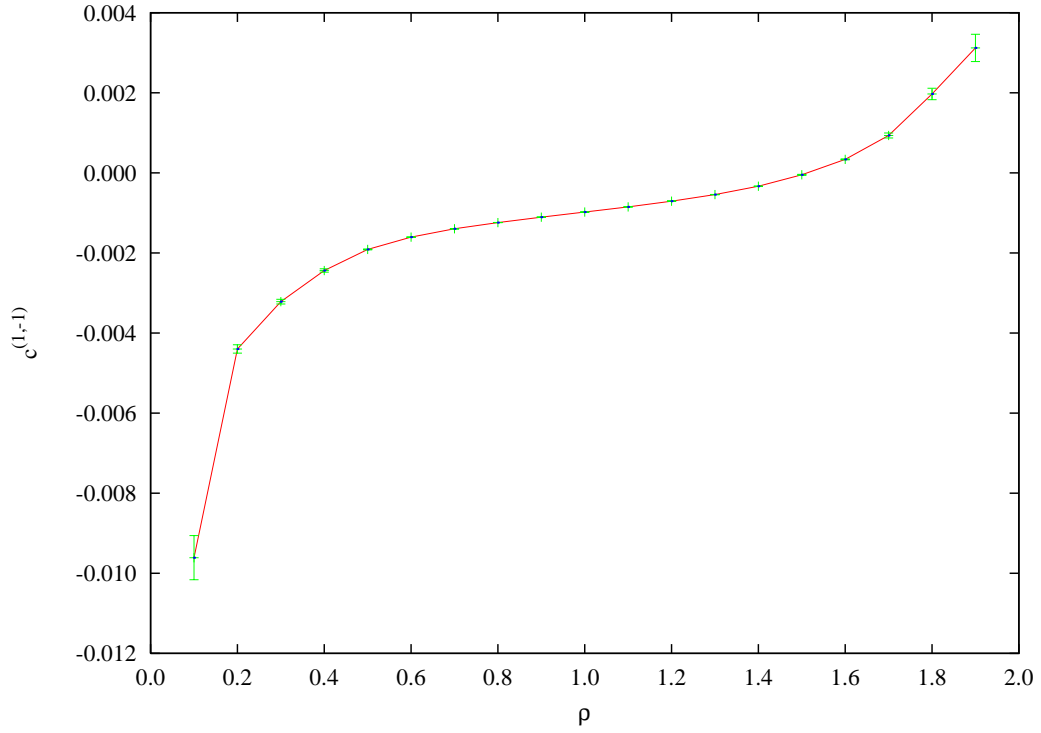


Fig. 4: Plot of the total 2-loop coefficient $c^{(1,-1)} \equiv \sum_i c_i^{(1,-1)}$ versus ρ .

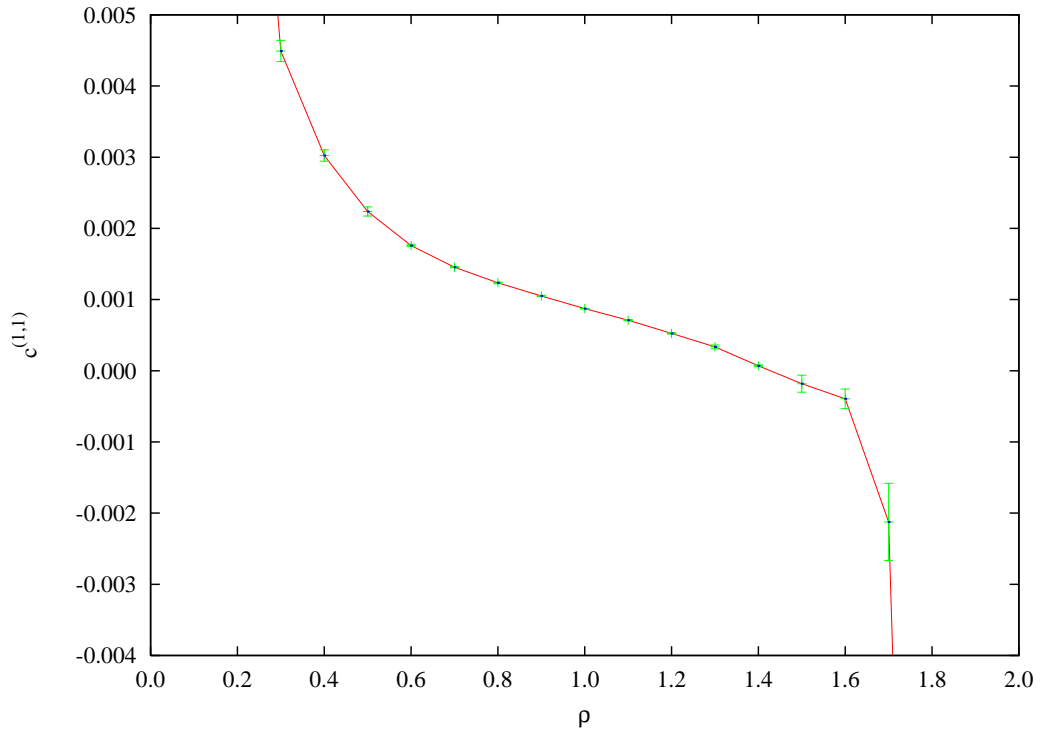


Fig. 5: Plot of the total 2-loop coefficient $c^{(1,1)} \equiv \sum_i c_i^{(1,1)}$ versus ρ .

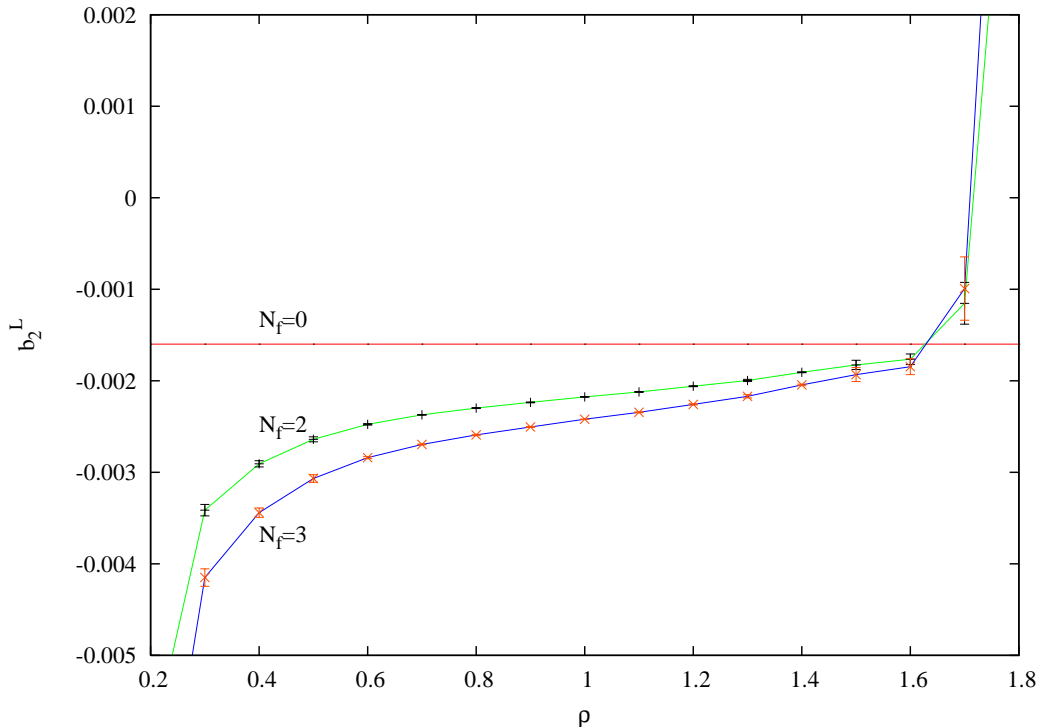


Fig. 6: The 3-loop coefficient b_2^L (Eq. (51)), plotted against ρ , for $N = 3$ and $N_f = 0$ (horizontal red line), $N_f = 2$ (green line) and $N_f = 3$ (blue line).

V. SUMMARY AND CONCLUSIONS

We have calculated the 2-loop coefficient of the coupling renormalization function Z_g , for the Yang-Mills theory with gauge group $SU(N)$ and N_f species of overlap fermions. We used the background field method to simplify the computation; in this method there is no need of evaluating any 3-point functions. This is the first 2-loop calculation using overlap fermions with external momenta, and it proved to be extremely demanding in human and CPU time; this is due to the fact that we had to manipulate very large expressions (millions of terms) in intermediate stages.

We used our numerical results of Z_g to determine the 3-loop coefficient b_2^L of the bare lattice β -function; the latter dictates the asymptotic dependence between the bare coupling constant g_0 and the lattice spacing a , required to maintain the renormalized coupling at a given scale fixed. Knowledge of b_2^L provides the correction term to the standard asymptotic scaling relation between a and g_0 , via Eq. (13).

The dependence of Z_g and b_2^L on N and N_f is shown explicitly in our expressions. On the other hand, dependence on the overlap parameter ρ cannot certainly be given in closed form; instead, we present our results for a large set of values of ρ in its allowed range.

The 3-loop correction is seen to be rather small: This indicates that the perturbative series is very well behaved in this case, despite the fact that it is only asymptotic in nature. Furthermore, around the values of ρ which are most often used in simulations ($1 \leq \rho \leq 1.6$), fermions bring about only slight corrections to the 3-loop β -function, even compared to pure

gluonic contributions, as can be seen from Fig. 6.

The only source of numerical error in our results has its origin in an extrapolation to infinite lattice size. Compatibly with the severe CPU constraints, numerical 2-loop integration had to be performed on lattices typically as large as 28^4 , or even up to 46^4 in cases where an improved extrapolation was called for. An intermediate range for ρ ($0.6 \leq \rho \leq 1.3$) showed the most stable extrapolation error, and this may be a sign of their suitability for numerical simulations.

As a by product of the present work, we have produced the lengthy expressions corresponding to *all* overlap vertices which can arise in a 2-loop computation, and presented them in a rather compact form. Further computations of similar complexity, for example the 2-loop renormalization of operators in the overlap action (such as fermion currents), only require the vertices which we have presented here.

Acknowledgements: This work is supported in part by the Research Promotion Foundation of Cyprus (Proposal Nr: ENISX/0505/45).

TABLES

ρ	$k^{(1)}$
0.1	0.020377(7)
0.2	0.01581702(2)
0.3	0.0133504717(2)
0.4	0.0116910952(1)
0.5	0.0104621922(2)
0.6	0.0095058191(2)
0.7	0.00874441051(7)
0.8	0.00813753230(4)
0.9	0.00766516396(3)
1.0	0.00732057894(3)
1.1	0.00710750173(2)
1.2	0.00703970232(7)
1.3	0.0071425543(2)
1.4	0.0074569183(2)
1.5	0.0080467046(1)
1.6	0.0090134204(1)
1.7	0.010526080(2)
1.8	0.0128914(2)
1.9	0.01680(8)

TABLE I. Coefficient $k^{(1)} \equiv \sum_i k_i^{(1)}$ for different values of the overlap parameter ρ .

ρ	$c^{(1,-1)}$	$c^{(1,1)}$
0.1	-0.0096(6)	0.124(3)
0.2	-0.0044(1)	0.0118(5)
0.3	-0.00321(6)	0.0045(1)
0.4	-0.00244(4)	0.0030(1)
0.5	-0.00191(1)	0.0022(6)
0.6	-0.001606(6)	0.00176(2)
0.7	-0.001397(3)	0.00145(1)
0.8	-0.001241(1)	0.00124(1)
0.9	-0.001107(1)	0.001051(9)
1.0	-0.000979(1)	0.000872(3)
1.1	-0.000849(2)	0.000710(8)
1.2	-0.000706(3)	0.00052(1)
1.3	-0.000543(4)	0.00033(3)
1.4	-0.000335(7)	0.00007(1)
1.5	-0.00005(1)	-0.0002(1)
1.6	0.00034(1)	-0.0004(1)
1.7	0.00093(6)	-0.0021(5)
1.8	0.0020(1)	-0.02(3)

TABLE II. Numerical results for the 2-loop coefficients $c^{(1,-1)} \equiv \sum_i c_i^{(1,-1)}$ and $c^{(1,1)} \equiv \sum_i c_i^{(1,1)}$

APPENDIX A: CONSTRUCTION OF VERTICES

Here we will explain the basic idea of expanding the expressions $1/\sqrt{X^\dagger X}$, appearing in the overlap-Dirac operator, in powers of g_0 , using a procedure introduced by Y. Kikukawa and A. Yamada [35]. We also provide the expression for $V_4^4(k_1, k_2)$ further below.

In an integral representation, the combination $\frac{1}{\sqrt{X^\dagger X}}$ can be written as

$$\frac{1}{\sqrt{X^\dagger X}} = \int_{-\infty}^{\infty} \frac{dt}{\pi} \frac{1}{t^2 + X^\dagger X} \quad (\text{A1})$$

In fact, Eq. (A1) is valid for any operator X provided that $X^\dagger X$ has no vanishing eigenvalues. We begin the desired expansion of the overlap-Dirac operator in powers of g_0 , by setting

$$X^\dagger X = \underbrace{X_0^\dagger X_0}_{\mathcal{O}(g_0^0)} + Z \quad (\text{A2})$$

The first term of Eq. (A2) corresponds to the inverse fermionic propagator, while Z leads to the vertices; for our 2-loop calculation we need to write Z up to $\mathcal{O}(g_0^4)$

$$\begin{aligned} Z = & \underbrace{(X_0^\dagger X_1 + X_1^\dagger X_0)}_{\mathcal{O}(g_0^1)} + \underbrace{(X_0^\dagger X_2 + X_1^\dagger X_1 + X_2^\dagger X_0)}_{\mathcal{O}(g_0^2)} + \underbrace{(X_0^\dagger X_3 + X_1^\dagger X_2 + X_2^\dagger X_1 + X_3^\dagger X_0)}_{\mathcal{O}(g_0^3)} \\ & + \underbrace{(X_0^\dagger X_4 + X_1^\dagger X_3 + X_2^\dagger X_2 + X_3^\dagger X_1 + X_4^\dagger X_0)}_{\mathcal{O}(g_0^4)} + \mathcal{O}(g_0^5) \end{aligned} \quad (\text{A3})$$

Using the above equations, we write the denominator on the r.h.s. of Eq. (A1) as

$$\frac{1}{t^2 + X^\dagger X} = \frac{1}{t^2 + X_0^\dagger X_0} \left(1 - Z \frac{1}{t^2 + X_0^\dagger X_0} + Z \frac{1}{t^2 + X_0^\dagger X_0} Z \frac{1}{t^2 + X_0^\dagger X_0} + \dots \right) \quad (\text{A4})$$

From this point forward it is easier to work in momentum space since, taking the Fourier transform, the denominator becomes diagonal

$$F.T. \left[\frac{1}{t^2 + X_0^\dagger X_0} \right] = \frac{1}{t^2 + \omega^2(p)} \quad (\text{A5})$$

($\omega^2(p)$ defined in Eq. (38)). Combining Eqs. (A1) and (A4) we derive the Taylor expansion of $\frac{1}{\sqrt{X^\dagger X}}$ in momentum space

$$\begin{aligned} \frac{1}{\sqrt{X^\dagger X}}_{F.T.}(p', p) = & \int_{-\infty}^{\infty} \frac{dt}{\pi} \frac{2\pi\delta(p' - p)}{t^2 + \omega^2(p')} - \int_{-\infty}^{\infty} \frac{dt}{\pi} \frac{1}{t^2 + \omega^2(p')} Z(p', p) \frac{1}{t^2 + \omega^2(p)} \\ & + \int_{-\infty}^{\infty} \frac{dt}{\pi} \int_{-\infty}^{\infty} \frac{dk}{(2\pi)^4} \frac{1}{t^2 + \omega^2(p')} Z(p', k) \frac{1}{t^2 + \omega^2(k)} Z(k, p) \frac{1}{t^2 + \omega^2(p)} + \dots \end{aligned} \quad (\text{A6})$$

The integral over t can now be performed by closing the contour around the upper complex t -plane. Considering, as an example the third term on the r.h.s. of Eq. (A6), the result is

$$\int_{-\infty}^{\infty} \frac{dt}{\pi} \frac{1}{t^2 + \omega^2(p')} \frac{1}{t^2 + \omega^2(k)} \frac{1}{t^2 + \omega^2(p)} = \frac{\omega(p') + \omega(k) + \omega(p)}{\omega(p')\omega(k)\omega(p) [\omega(p') + \omega(k)] [\omega(k) + \omega(p)] [\omega(p) + \omega(p')]}$$

Similarly we integrate all terms of Eq. (A6) over t and this leads to Eqs. (38)-(42) and to the expression for $V_4^4(k_1, k_2)$ which is presented below

$$\begin{aligned} V_4^4(k_1, k_2) = & \int \int \int \frac{d^4 k_3}{(2\pi)^4} \frac{d^4 k_4}{(2\pi)^4} \frac{d^4 k_5}{(2\pi)^4} \frac{1}{12} \left(\prod_{p \in S_5} \frac{1}{\omega(k_{p_1}) + \omega(k_{p_2})} \right) \times \\ & \left[\left(\sum_{p \in S_5} \omega(k_{p_1}) \omega(k_{p_2}) \omega(k_{p_3}) \omega(k_{p_4}) \left(\omega(k_{p_1})/6 + \omega(k_{p_5})/30 \right) \right) \times \right. \\ & \left[(X_1(k_1, k_3) X_1^\dagger(k_3, k_4) X_1(k_4, k_5) X_1^\dagger(k_5, k_2) \chi_0(k_2) \right. \\ & + X_1(k_1, k_3) X_1^\dagger(k_3, k_4) X_1(k_4, k_5) \chi_0^\dagger(k_5) X_1(k_5, k_2) \\ & + X_1(k_1, k_3) X_1^\dagger(k_3, k_4) \chi_0(k_4) X_1^\dagger(k_4, k_5) X_1(k_5, k_2) \\ & + X_1(k_1, k_3) \chi_0^\dagger(k_3) X_1(k_3, k_4) X_1^\dagger(k_4, k_5) X_1(k_5, k_2) \\ & \left. \left. + \chi_0(k_1) X_1^\dagger(k_1, k_3) X_1(k_3, k_4) X_1^\dagger(k_4, k_5) X_1(k_5, k_2) \right] \right. \\ & \left. - \frac{1}{6} \left(\sum_{p \in S_5} \omega(k_{p_1}) \omega(k_{p_2}) \left(\omega(k_{p_1}) + \omega(k_{p_3}) \right) \right) \times \right. \\ & \left[X_1(k_1, k_3) \chi_0^\dagger(k_3) X_1(k_3, k_4) X_1^\dagger(k_4, k_5) \chi_0(k_5) X_1^\dagger(k_5, k_2) \chi_0(k_2) \right. \\ & + X_1(k_1, k_3) \chi_0^\dagger(k_3) X_1(k_3, k_4) \chi_0^\dagger(k_4) X_1(k_4, k_5) \chi_0^\dagger(k_5) X_1(k_5, k_2) \\ & + X_1(k_1, k_3) \chi_0^\dagger(k_3) X_1(k_3, k_4) \chi_0^\dagger(k_4) X_1(k_4, k_5) X_1^\dagger(k_5, k_2) \chi_0(k_2) \\ & + X_1(k_1, k_3) X_1^\dagger(k_3, k_4) \chi_0(k_4) X_1^\dagger(k_4, k_5) \chi_0(k_5) X_1^\dagger(k_5, k_2) \chi_0(k_2) \\ & + \chi_0(k_1) X_1^\dagger(k_1, k_3) \chi_0(k_3) X_1^\dagger(k_3, k_4) \chi_0(k_4) X_1^\dagger(k_4, k_5) X_1(k_5, k_2) \\ & + \chi_0(k_1) X_1^\dagger(k_1, k_3) \chi_0(k_3) X_1^\dagger(k_3, k_4) X_1(k_4, k_5) \chi_0^\dagger(k_5) X_1(k_5, k_2) \\ & + \chi_0(k_1) X_1^\dagger(k_1, k_3) \chi_0(k_3) X_1^\dagger(k_3, k_4) X_1(k_4, k_5) X_1^\dagger(k_5, k_2) \chi_0(k_2) \\ & + \chi_0(k_1) X_1^\dagger(k_1, k_3) X_1(k_3, k_4) \chi_0^\dagger(k_4) X_1(k_4, k_5) \chi_0^\dagger(k_5) X_1(k_5, k_2) \\ & + \chi_0(k_1) X_1^\dagger(k_1, k_3) X_1(k_3, k_4) \chi_0^\dagger(k_4) X_1(k_4, k_5) X_1^\dagger(k_5, k_2) \chi_0(k_2) \\ & \left. \left. + \chi_0(k_1) X_1^\dagger(k_1, k_3) X_1(k_3, k_4) X_1^\dagger(k_4, k_5) \chi_0(k_5) X_1^\dagger(k_5, k_2) \chi_0(k_2) \right] \right. \\ & \left. + \left(\sum_{p \in S_5} \frac{\omega^2(k_{p_1}) \omega(k_{p_2}) \omega(k_{p_3})}{\omega(k_1) \omega(k_2) \omega(k_3) \omega(k_4) \omega(k_5)} \times \right. \right. \\ & \left. \left. \left(\omega(k_{p_2}) [\omega(k_{p_1})/2 + \omega(k_{p_3})/6] + \omega(k_{p_4}) [\omega(k_{p_1})/3 + \omega(k_{p_2}) + \omega(k_{p_5})/3] \right) \right) \times \right. \\ & \left. \left. \chi_0(k_1) X_1^\dagger(k_1, k_3) \chi_0(k_3) X_1^\dagger(k_3, k_4) \chi_0(k_4) X_1^\dagger(k_4, k_5) \chi_0(k_5) X_1^\dagger(k_5, k_2) \chi_0(k_2) \right] \right. \end{aligned} \quad (A7)$$

(S_5 : permutation group of the numbers 1 through 5)

REFERENCES

- [1] R. Narayanan, H. Neuberger, Phys. Rev. Lett. **71** (1993) 3251, [hep-lat/9308011]
- [2] H. Neuberger, Phys. Lett. **B 417** (1998) 141 ; **B 427** (1998) 353, [hep-lat/9707022]; [hep-lat/9801031]
- [3] H. Neuberger, Ann. Rev. Nucl. Part. Sci. **51** (2001) 23, [hep-lat/0101006]
- [4] D.B. Kaplan, Phys. Lett. **B288** (1992) 342, [hep-lat/9206013]
- [5] V. Furman, Y. Shamir, Nucl. Phys. **B439** (1995) 54, [hep-lat/9405004]
- [6] T. DeGrand, Z. Liu, S. Schaefer, Phys. Rev. **D74** (2006) 099904, [hep-lat/0608019]
- [7] E.-M. Ilgenfritz, K. Koller, Y. Koma, G. Schierholz, T. Streuer, V. Weinberg, Phys. Rev. **D76** (2007) 034506, [arXiv:0705.0018]
- [8] J. Bloch, A. Frommer, B. Lang, T. Wettig, arXiv:0704.3486
- [9] JLQCD collaboration: H. Fukaya et al., hep-lat/0702003
- [10] R. Babich, N. Garron, C. Hoelbling, J. Howard, L. Lellouch, C. Rebbi, hep-lat/0701023
- [11] O. Bär, K. Jansen, S. Schaefer, L. Scorzato, A. Shindler, hep-lat/0609039
- [12] T. Draper, N. Mathur, J. Zhang, A. Alexandru, Y. Chen, S.-J. Dong, I. Horvath, F.X. Lee, K.-F. Liu, S. Tamhankar, hep-lat/0609034
- [13] M. Göckeler, R. Horsley, H. Perlt, P.E.L. Rakow, G. Schierholz, A. Schiller, PoS(LAT2006)161, [hep-lat/0610060]
- [14] M. Ioannou, H. Panagopoulos, Phys. Rev. **D73** (2006) 054507, [hep-lat/0601020]
- [15] T. DeGrand, Phys. Rev. **D67** (2003) 014507, [hep-lat/0210028]
- [16] S. Capitani, Nucl. Phys. Proc. Suppl. **106** (2002) 826, [hep-lat/0108028]
- [17] S. Capitani, L. Giusti, Phys. Rev. **D62** (2000) 114506, [hep-lat/0007011]
- [18] C. Alexandrou, E. Follana, H. Panagopoulos, E. Vicari, Nucl. Phys. **B580** (2000) 394, [hep-lat/0002010]
- [19] C. Alexandrou, H. Panagopoulos, E. Vicari, Nucl. Phys. **B571** (2000) 257, [hep-lat/9909158]
- [20] A. Skouroupathis, H. Panagopoulos, Phys. Rev. **D72** (2005) 094509, [hep-lat/0509012]
- [21] A. Athenodorou, H. Panagopoulos, Phys. Rev. **D70** (2004) 077507, [hep-lat/0408020]
- [22] A. Hasenfratz, P. Hasenfratz, Nucl. Phys. **B193** (1981) 210
- [23] M. Lüscher and P. Weisz, Nucl. Phys. **B452** (1995) 234, [hep-lat/9505011]
- [24] C. Christou, A. Feo, H. Panagopoulos, E. Vicari, Nucl. Phys. **B525** (1998) 387, [hep-lat/9801007]
- [25] A. Bode, H. Panagopoulos, Nucl. Phys. **B625** (2002) 198-210, [hep-lat/110211]
- [26] A. Bode, H. Panagopoulos, Y. Proestos, Nucl. Phys. Proc. Suppl. **106** (2002) 832, [hep-lat/0110225]
- [27] O.V. Tarasov, A.A. Vladimirov, A. Zharkov, Phys. Lett. **B98** (1980) 429
- [28] Q. Mason, H.D. Trottier, C.T.H. Davies, K. Foley, A. Gray, G. P. Lepage, M. Nobes, J. Shigemitsu, Phys. Rev. Lett. **95** (2005) 052002, [hep-lat/0503005]
- [29] R. Sommer, Lectures given at ILFTN Workshop on Perspectives in Lattice QCD, Nara, Japan, October 2005, [hep-lat/0611020]
- [30] ALPHA Collaboration: M. Della Morte, R. Frezzotti, J. Heitger, J. Rolf, R. Sommer, U. Wolff, Nucl. Phys. **B713** (2005) 378, [hep-lat/0411025]
- [31] O. Kaczmarek, F. Karsch, P. Petreczky, F. Zantow, Phys. Rev. **D70** (2004) 074505; Erratum-ibid. **D72** (2005) 059903, [hep-lat/0406036]
- [32] L.F. Abbott, Nucl. Phys. **B185** (1981) 189
- [33] R. K. Ellis, G. Martinelli, Nucl. Phys. **B235** (1984) 93
- [34] B. Allés, A. Feo, H. Panagopoulos, Nucl. Phys. **B491** (1997) 498, [hep-lat/9609025]
- [35] Y. Kikukawa, A. Yamada, Nucl. Phys. **B547** (1999) 413, [hep-lat/9808026]